

SYNCHRONIZATION CONDITIONS OF COUPLED MAPS USING PERIODICITIES

R. O. E. Bustos–Espinoza^{1,a} and G. M. Ramírez–Ávila^{1,b}

Instituto de Investigaciones Físicas, Casilla 8635, Universidad Mayor de San Andrés, La Paz, Bolivia.

Abstract. Using the synchrony factor and its periodicity, we are able to identify not only complete synchronization but also in-phase synchronization. The analysis of the periodicities of the synchrony factor allows to obtain a phase diagram that contains all the information of synchronous behavior in a wide range of parameters. This method constitutes a new and useful tool to study synchronization.

1 Introduction

The study of dynamic systems and the establishment of general properties of those systems have been favored by the inclusion of mathematical objects describing a discrete dynamics called maps. Among the most well known maps, we can mention the logistic map introduced by May [1] and the Hénon map [2]. An important feature of nonlinear maps is the fact that they can give rise to chaotic behavior even in one-dimensional maps as in the case of logistic ones.

Many works have been devoted to the understanding of dynamical properties of maps as is shown by Kaneko in his study of period-adding phenomena in one-dimensional mapping where he showed frequency-locking by extending the theory of intermittency [3] and the measuring of transient chaos in one- and two-dimensional maps [4]. Interesting phenomena were described in coupled map lattices, especially in logistic maps, such as the transition from torus to chaos accompanied by frequency locking with symmetry breaking [5], and the period-doubling of kink-antikink patterns of a one-dimensional lattice [6]; the Lyapunov analysis and information flow [7], and the spatiotemporal chaos related to Bénard convection [8].

A traditional approach to study dynamical systems consists in performing linear stability and bifurcation analysis complemented by the obtention of Lyapunov exponents, a tool that allows to determine the regular or chaotic behavior of a system. Full-extent analysis of dynamical systems by means of parameter spaces characterized by Lyapunov exponents [9] constitutes a useful technique that allowed to unravel the dynamical behavior of diverse nature systems such as physical [10], chemical [11], and biological [9] among others.

Recently, the analysis of parameter spaces by means of periodicities turns out to be more appropriate cause it provides not only the determination of whether or not a system is regular but a deeper insight on the dynamical properties [12,13,14]

^a e-mail: robustos@umsa.bo

^b e-mail: gramirez@ulb.ac.be

Synchronization is a ubiquitous phenomenon in nature deserving the interest of scientist of different branches, going from physics [15] to social sciences [16].

Synchronization in coupled maps has been widely studied in different contexts; for instance, considering parameter mismatch and noise [17]; or giving prescribed synchronized dynamics on globally coupled systems [18,19]; or the description of partial [20] and anticipated synchronization [21].

This work is organized as follows: In Sect. 2, we point out the main features of the consider system, namely, the coupled logistic maps; we also describe the coupling conditions and the characterization of synchronous behavior. In Sect.3, we show the obtained parameter spaces characterized by the periodicities using the coupling strength and the parameter mismatch. Finally, in Sect. 4 we give the conclusions and perspectives of this research.

2 Model

For our study we use as a model diffusively coupled logistic maps [6], given by:

$$x_{n+1}^{(i)} = \mu^{(i)} x_n^{(i)} (1 - x_n^{(i)}) + \sum_{\substack{i,j \\ i \neq j}}^N \beta_{ij} (x_n^{(j)} - x_n^{(i)}), \quad (i, j = 1, \dots, N) \quad , \quad (1)$$

where superscripts identify the oscillators, subscripts represent their evolution, β_{ij} denotes the coupling strength, i.e., the action of oscillator j on oscillator i and $x_n^{(i)}$ is the dynamical variable of oscillator i and it is defined in $[0, 1]$. For computational purposes we impose the conditions:

$$\begin{aligned} \text{If } x_n &\geq 1 &\Rightarrow & x_n = 1 \\ \text{If } x_n &\leq 0 &\Rightarrow & x_n = 0 \end{aligned}$$

In order to characterize the synchronization, we introduce the synchrony factor σ defined as:

$$\sigma_n = |x_n^{(2)} - x_n^{(1)}| \quad , \quad (2)$$

which allows us to identify different types of synchrony, such as:

- Complete synchronization when $\sigma_n \rightarrow 0$.
- Anti-synchronization when $\sigma_n \rightarrow 1$.
- Phase synchronization when σ_n oscillates with well-defined periods.

Several works have been devoted to synchronization on coupled maps using σ_n [22], as the quantity to characterize synchronization; nevertheless, none consider the situation in which σ_n oscillates periodically.

With the aim of featuring phase synchronization, we consider a system composed of two coupled logistic maps:

$$\begin{aligned} x_{n+1}^{(1)} &= (\mu^{(1)} + \frac{\Delta\mu}{2}) x_n^{(1)} (1 - x_n^{(1)}) + \beta (x_n^{(2)} - x_n^{(1)}) \\ x_{n+1}^{(2)} &= (\mu^{(2)} - \frac{\Delta\mu}{2}) x_n^{(2)} (1 - x_n^{(2)}) + \beta (x_n^{(1)} - x_n^{(2)}) \end{aligned} \quad (3)$$

For this system, we obtain the parameter space, coupling strength β vs. parameter mismatch $\Delta\mu$, exhibiting synchronous regions in terms of the periodicities of σ_n (σ -periodicities).

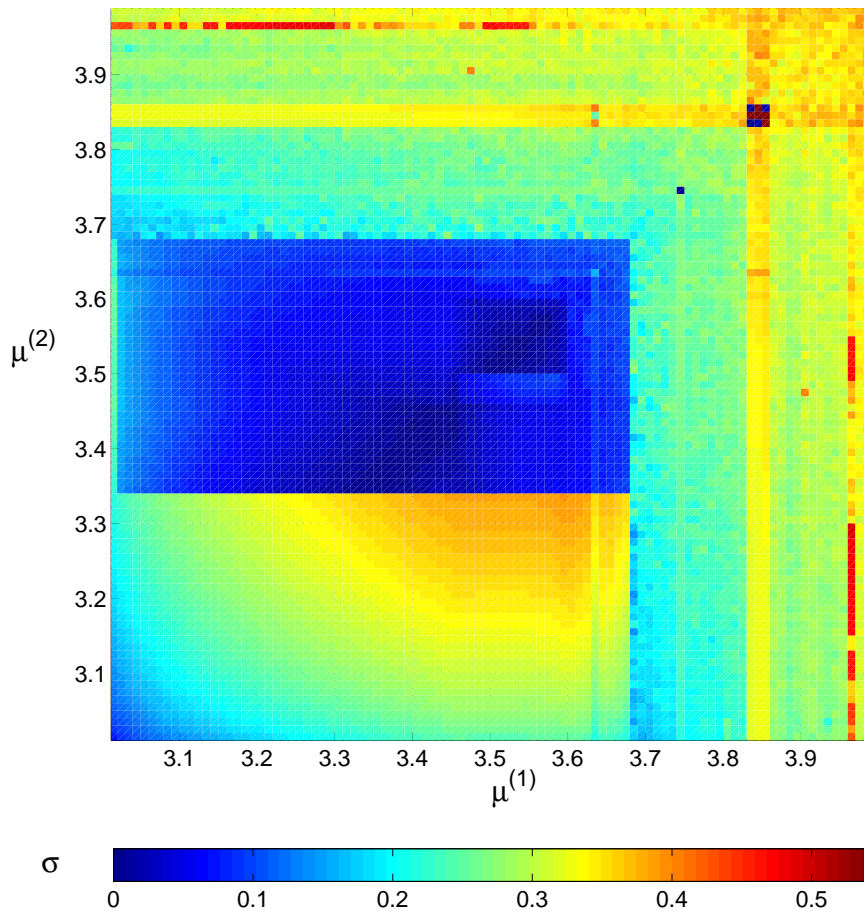


Fig. 1. (Color online) Parameter space in the plane $(\mu^{(1)}, \mu^{(2)})$ in terms of synchrony factor σ (color bar), after $n = 10^5$ time steps for two coupled logistic maps defined in the interval $3 \leq \mu^{(i)} \leq 4$ and being $\beta = 0.003$.

3 Results

Using the model and the conditions described in Sect. 2, we study the synchronous behavior of the system by means of the parameter space characterized by the synchronization factor σ computed taking the mean over the last 500 values (see Fig. 1). The diagram has been obtained after $n = 10^5$ time steps and considering a coupling strength $\beta = 0.003$. The parameters $\mu^{(i)}$, $(i = 1, 2)$ are defined in the interval $[3, 4]$; thus, the maps can exhibit regular or chaotic behavior.

From Fig. 1 we choose the point $\mu^{(1)} = \mu^{(2)} = 3.83$ for which $\sigma \approx 0$; it is noteworthy to mention that for this value of σ , the map behaves regularly with period 3 when it is not coupled; on the other hand, when the maps are coupled, they synchronize and the behavior is in general regular but with a change in their period. The latter enables us to describe synchronization in the phase diagram β vs. $\Delta\mu$ as shown in

Fig. 2a, where the color code is based on the value of the synchronization factor σ . A magnification of the central part where $\sigma \approx 0$ is shown in Fig. 2b, (see also [23]).

From Fig. 2b, we observe clearly that for small coupling strength values, synchronization is not achieved. For $\beta \approx 0,002$ the system completely synchronizes even if the oscillators are different with a mismatch $\Delta\mu \approx 0.004$. The region of complete synchronization becomes narrower with the increase of the coupling strength, in opposition to what usually happens with Arnold tongues. Complete synchronization is possible until the coupling attains a value $\beta \approx 0.037$.

3.1 Analysis of Periodicities

The analysis of Fig. 2a shows interesting findings such as the identification of a region of complete synchronization and the presence of some symmetric regions that exhibit constant mean values of σ . Nevertheless, the precedent information does not tell us any information on the dynamics of the oscillators. In order to have a deeper insight of what reflects those symmetric regions, we choose some points inside the regions from which we obtain the evolution of the dynamic variables $x^{(i)}$ and σ as shown in Figs. 3a–e and in Figs. 3f–j respectively.

From Figs. 3a–e we note that the signals are synchronized in phase and this fact is reflected by the periodic behavior of illustrated in Figs. 3f–j. The latter indicates us that these regions are linked to in-phase synchronous behavior and they deserve a complementary study in terms of periodicities.

An exhaustive numerical computation of periodicities of Fig. 2 permits us to obtain a new phase diagram (see Fig. 4) but now, in terms of σ -periodicities instead of σ simply. The inspection of Fig. 4 shows us that the symmetric regions appearing in Fig. 2, are also present in Fig. 4 but characterized by well-defined values of periodicity. With the aim of having a better approach of the above mentioned regions, we identify each of these by means of a rectangle and a capital letter. In Fig. 5, we magnify some of these regions in order to see with more detail the involved periodicities. We can point out some interesting features appearing in these regions, e.g., the almost perfect symmetry both in their shapes and in their σ -periodicities values. It is interesting to note that each region exhibits several values of σ -periodicity. Thus, the larger regions of Fig. 4 show σ -periodicities 3, 6, 12, ...; in all the panels of Fig. 5 the σ -periodicities are 5, 10, 20, ... The latter results is an indication of a periodic behavior that follows a chaotic one.

In Fig. 6, we verify the exactness of the information obtained from Fig. 5 in which concerns the σ -periodicities, i.e., we represent the time series corresponding to the dynamic variables $x^{(1)}$ and $x^{(2)}$ that are clearly synchronized in phase (Figs. 6a–f). Similarly, the evolution of σ is represented in Figs. 6g–l and the corresponding periodicities coincide with those shown in Figs. 4 and 5.

The periodicities P of the synchrony factor σ (σ -periodicities) are computed by determining how many time steps are necessary in the time series of σ for finding a repetitive situation.

Even though, the analysis has been made for a situation in which the uncoupled maps behave as periodic, we can also carry out numerical experiments for μ values of the map corresponding to a chaotic behavior ($\mu = 3.78$). The coupled maps once again synchronize and as a consequence it is possible to find the corresponding σ -periodicity P as shown in Fig. 7

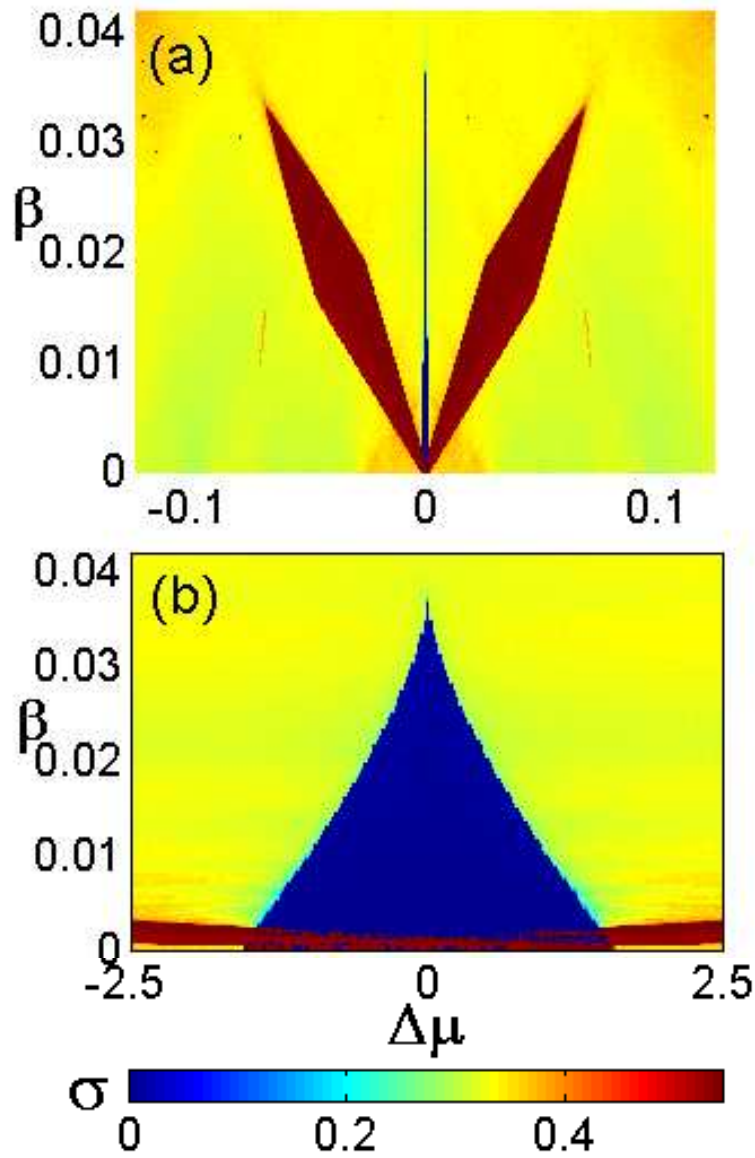


Fig. 2. (Color online) (a) Synchronization region in the plane coupling strength (β) vs. parameter mismatch ($\Delta\mu$), where $\mu^{(1)} = \mu^{(2)} = 3.83$. (b) Magnification of the central triangular region, where $\sigma \approx 0$ [23]. The color code for both is the same and is similar to that used in Fig. 1

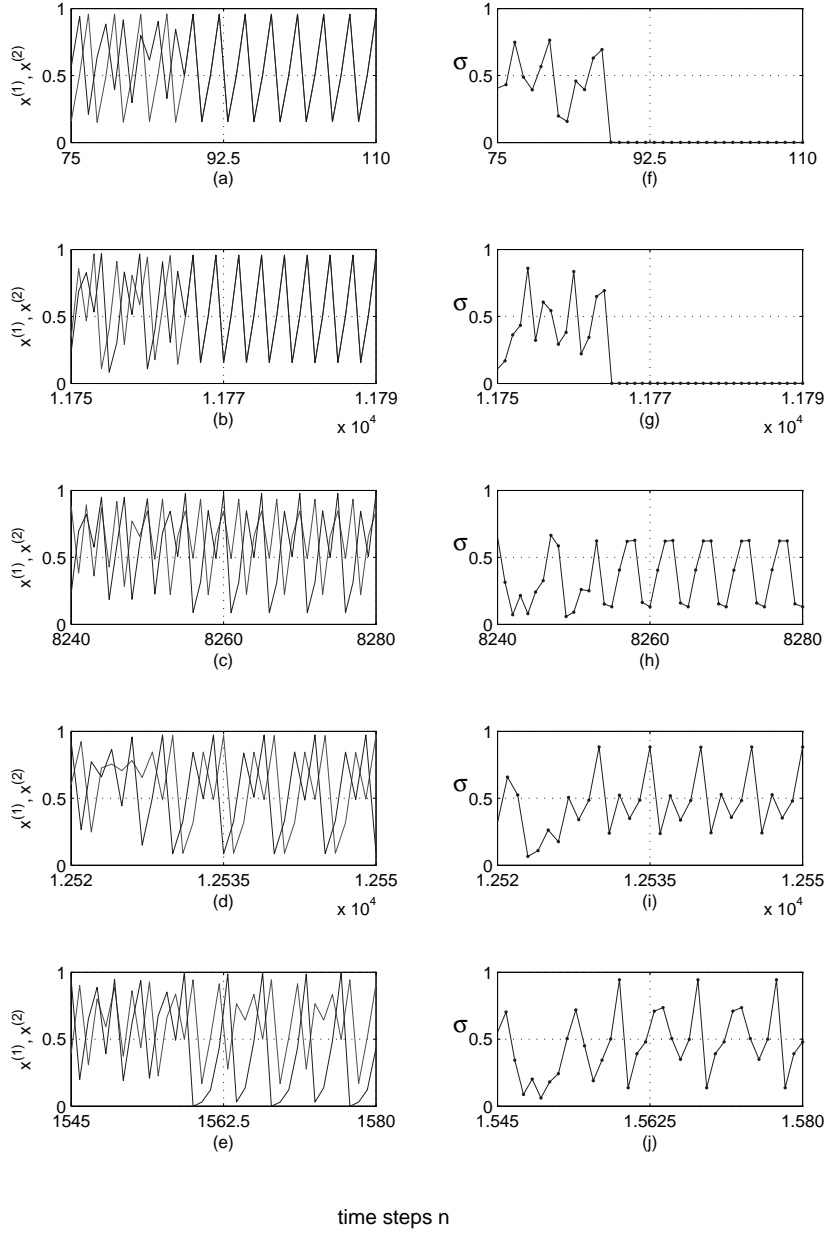


Fig. 3. Time series of (a)–(e) variables $x^{(1)}$ (black) and $x^{(2)}$ (gray), and (f)–(j) synchrony factor σ : (a) and (f): $\Delta\mu = -1.151 \times 10^{-6}$, $\beta = 3.003 \times 10^{-3}$, complete synchronization; (b) and (g): $\Delta\mu = -1.151 \times 10^{-6}$, $\beta = 3.641 \times 10^{-2}$, complete synchronization; (c) and (h): $\Delta\mu = -7.025 \times 10^{-2}$, $\beta = 1.216 \times 10^{-2}$, $P = 20$; (d) and (i): $\Delta\mu = -1.838 \times 10^{-2}$, $\beta = 3.226 \times 10^{-2}$, $P = 10$; (e) and (j): $\Delta\mu = -1.215 \times 10^{-6}$, $\beta = 3.240 \times 10^{-2}$, $P = 9$.

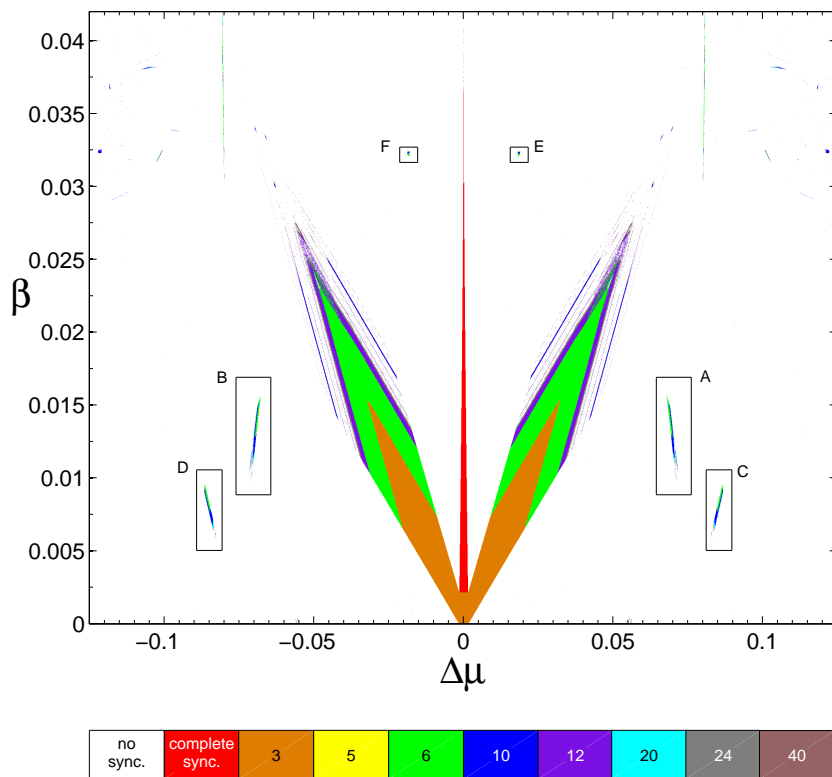


Fig. 4. (Color online) Phase diagram β vs. $\Delta\mu$ in terms of σ -periodicities. Each color indicates either the situation of non-synchronization (white), complete synchronization (red), or the values of the periodicity. The color bar represents the main periodicities appearing in the synchronization regions.

4 Conclusions and Perspectives

The main issue of this work is related to the finding of a new method to describe synchronization in coupled maps. This method is based on the determination of periodicities of the synchrony factor σ . These σ -periodicities allow us to identify not only complete synchronization (stable value of $\sigma \approx 0$) but also in-phase synchronization, where the σ -periodicities is an induction of a synchronous behavior of the system. We carried out extensive numerical computation in order to obtain a phase diagram (coupling strength, β vs. parameter mismatch, $\Delta\mu$) based on the values of σ -periodicities. This diagram contains information of the synchronous behavior in a wide range of parameters. The inspection of the phase diagram allowed us to identify several regions

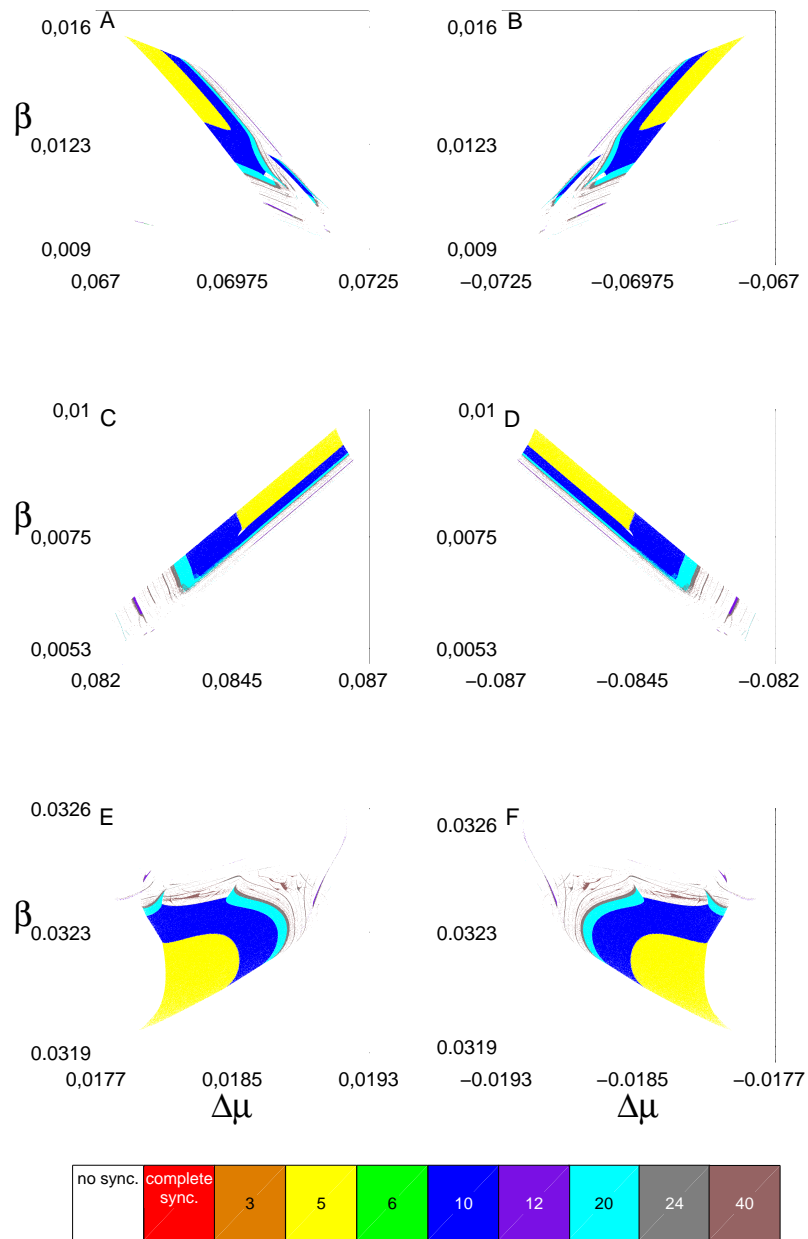


Fig. 5. (Color online) Zoom of some of the regions shown in Fig. 4. It is remarkable the symmetry both in their shapes and in their σ -periodicity values. As in Fig. 4, the color bar represents the main periodicities appearing in the synchronization regions where each color indicates either the situation of non-synchronization (white) or the σ -periodicity values. The main periodicity values are 5, 10, 20 and 40.

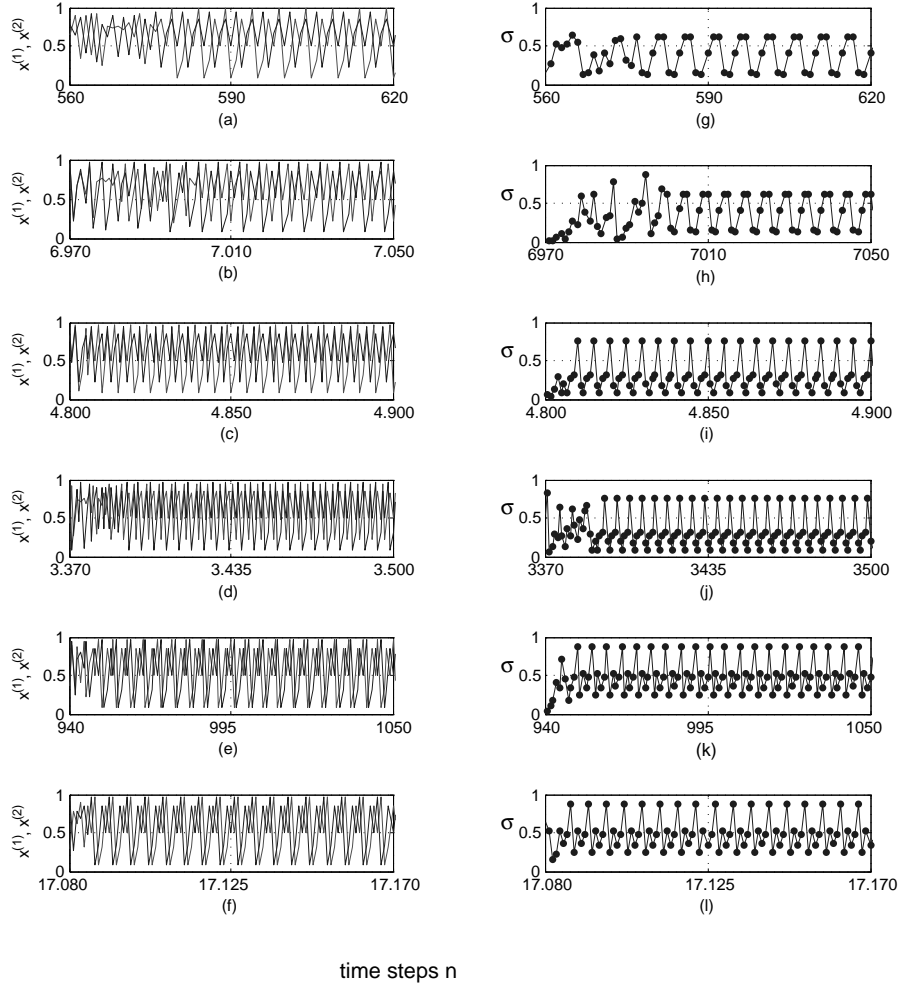


Fig. 6. Time series of (a)–(f) variables $x^{(1)}$ (black) and $x^{(2)}$ (gray), and (g)–(l) synchrony factor σ : (a) and (g): $\Delta\mu = 6.929 \times 10^{-2}$, $\beta = 1.318 \times 10^{-2}$, $P = 5$; (b) and (h): $\Delta\mu = -6.991 \times 10^{-2}$, $\beta = 1.250 \times 10^{-2}$, $P = 10$; (c) and (i): $\Delta\mu = 8.362 \times 10^{-2}$, $\beta = 6.784 \times 10^{-3}$, $P = 20$; (d) and (j): $\Delta\mu = -8.345 \times 10^{-2}$, $\beta = 6.877 \times 10^{-3}$, $P = 40$; (e) and (k): $\Delta\mu = 1.879 \times 10^{-2}$, $\beta = 3.233 \times 10^{-2}$, $P = 80$; (f) and (l): $\Delta\mu = -1.881 \times 10^{-2}$, $\beta = 3.232 \times 10^{-2}$, $P = 80$.

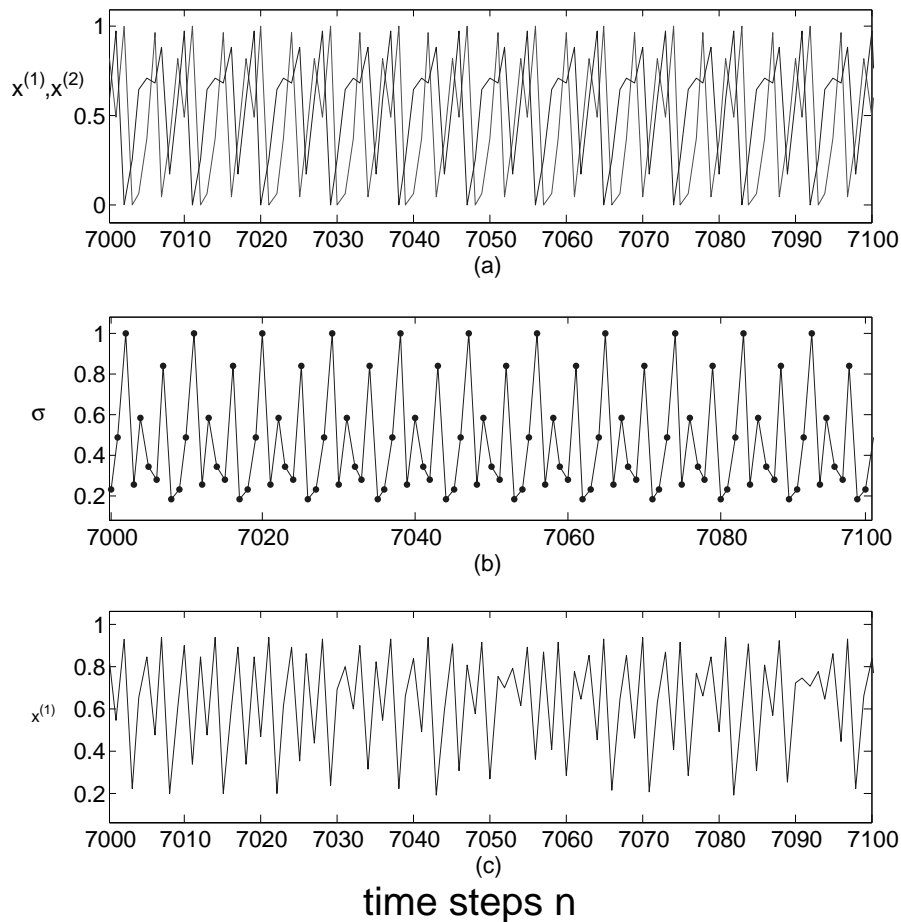


Fig. 7. (a) Time series for two coupled maps $x^{(1)}$ (black) and $x^{(2)}$ (gray) with the same value of $\mu = 3.78$ (chaotic one). (b) The time series of σ showing a periodical behavior $P = 9$. (c) A time series for a logistic map with the same μ value corresponding to a chaotic region.

in which in-phase synchronization is possible. A remarkable aspect of these regions are their symmetry both in shape and in σ -periodicity values.

Finally, these regions exhibit several σ -periodicities values, being the most common, the sequences 3, 6, 12, ... and 5, 10, 20, ..., which indicates that the periodic behavior observed in these regions followed a chaotic one.

This detailed characterization of the synchronization of two coupled maps might be very useful in systems containing a lot number of maps for which it is possible to consider distance-dependent coupling, and even time-varying coupling.

References

1. R. May, Nature **261**, 459 (1976)
2. M. Hénon, Commun. Math. Phys. **50**, 69 (1976)

3. K. Kaneko, Prog. Theor. Phys. **68**, 669 (1982)
4. K. Buszko, K. Stefanski, Chaos. Soliton. Fract. **27**, 630 (2006)
5. K. Kaneko, Prog.Theor. Phys. **69**, 1427 (1983)
6. K. Kaneko, Prog.Theor. Phys. **72**, 480 (1984)
7. K. Kaneko, Physica D **23**, 436 (1986)
8. K. Kaneko, Physica D **37**, 60 (1989)
9. J.A.C. Gallas, Int. J. Bifurcat. Chaos. **20**, 197 (2010)
10. C. Bonatto, G.J. C., J.A.C. Gallas, Phys. Rev. Lett. **95**, 143905 (2005)
11. J.G. Freire, R. Field, J.A.C. Gallas, J. Chem. Phys. **131**, 044105 ((2009))
12. J.A.C. Gallas, Phys. Rev. Lett. **70**, 2714 (1993)
13. J.A.C. Gallas, Phys. Rev. E **48**, R4156 (1993)
14. J.A.C. Gallas, Physica A **202**, 196 (1994)
15. A. Pikovsky, M. Rosenblum, J. Kurths, *Synchronization: a universal concept in nonlinear sciences* (Cambridge University Press, New York, 2001)
16. A. Stanoev, D. Smilkov, *Consensus and Synchronization in Complex Networks* (Springer, Macedonia, 2013)
17. O. Morgul, Phys. Lett. A **247**, 391 (1998)
18. D.H. Zanette, A. Mikhailov, Phys. Rev. E **57**, 276 (1998)
19. D.H. Zanette, Eur. Phys. J. B. **16**, 537 (2000)
20. A.V. Taborov, Y.L. Maistrenko, Int. J. Bifurcat. Chaos. **10**, 1051 (2000)
21. C. Masoller, D.H. Zanette, Physica A **300**, 359 (2001)
22. C. Masoller, A.C. Martí, Phys. Rev. Lett. **94**, 134102 (2005)
23. R.O.E. Bustos-Espinoza, G.M. Ramírez-Ávila, Rev. Bol. Fis. (**22**), 1 (2012)